An inverse cascade explanation for the power-law frequency–area statistics of earthquakes, landslides and wildfires

BRUCE D. MALAMUD[1] & DONALD L. TURCOTTE[2]

[1]*Environmental Monitoring and Modelling Research Group, Department of Geography, King's College London, Strand, London WC2R 2LS, UK (e-mail: bruce@malamud.com)*

[2]*Department of Geology, University of California, Davis, CA, 95616, USA (e-mail: turcotte@geology.ucdavis.edu)*

Abstract: Frequency–magnitude statistics for natural hazards can greatly help in probabilistic hazard assessments. An example is the case of earthquakes, where the generality of a power-law (fractal) frequency–rupture area correlation is a major feature in seismic risk mapping. Other examples of this power-law frequency–size behaviour are landslides and wildfires. In previous studies, authors have made the potential association of the hazard statistics with a simple cellular-automata model that also has robust power-law statistics: earthquakes with slider-block models, landslides with sandpile models, and wildfires with forest-fire models. A potential explanation for the robust power-law behaviour of both the models and natural hazards can be made in terms of an inverse-cascade of metastable regions. A metastable region is the region over which an 'avalanche' spreads once triggered. Clusters grow primarily by coalescence. Growth dominates over losses except for the very largest clusters. The cascade of cluster growth is self-similar and the frequency of cluster areas exhibits power-law scaling. We show how the power-law exponent of the frequency–area distribution of clusters is related to the fractal dimension of cluster shapes.

The frequency–size statistics of a number of natural hazards appear to satisfy power-law (fractal) scaling to a good approximation under a wide variety of conditions (for a review, see Malamud 2004). These include earthquakes (Aki 1981; Turcotte & Malamud 2002), volcanic eruptions (Pyle 2000), wildfires (Malamud *et al.* 1998, 2005; Ricotta *et al.* 1999), landslides (Guzzetti *et al.* 2002; Malamud *et al.* 2004), asteroid impacts (Chapman & Morrison 1994; Chapman 2004) and potentially floods (Turcotte & Greene 1993; Turcotte 1994; Malamud *et al.* 1996; Malamud & Turcotte 2006). In this paper, we will consider the frequency–area statistics of three of these natural hazards: earthquakes, landslides, and wildfires. In each case the 'noncumulative' number of events N with area A satisfies the power-law relation

$$N \sim A^{-\beta} \tag{1}$$

to a good approximation and over many orders of magnitude, where β is a constant. A number of simple cellular-automata models have also been shown to exhibit robust power-law behaviour (e.g. see Malamud & Turcotte 2000), including the slider-block, sandpile, and forest-fire models. In this paper we will first discuss the frequency–area statistics of earthquakes, landslides, and wildfires. We will then discuss the frequency–area statistics of the slider-block, sandpile, and forest-fire cellular-automata models. Finally, in the context of real wildfires and the forest-fire model, we will advance a potential explanation for the robust power-law behaviour of both in terms of an inverse-cascade of metastable regions.

Earthquakes

The first natural hazard that was recognized to exhibit power-law frequency–area statistics was earthquakes. For more than fifty years it has been accepted that the rate at which earthquakes occur in a region generally satisfies the Gutenberg–Richter (1954) frequency–magnitude relation

$$\log \dot{N}_{\mathrm{CE}} = -bM + \log \dot{a} \tag{2}$$

where $\dot{N}_{\mathrm{CE}}$ is the cumulative number of earthquakes with a magnitude greater than or equal to M in a specified area and time, and b and $\dot{a}$ are constants. Aki (1981) showed that Eq. (2) is equivalent to the power-law relation:

$$\dot{N}_{\mathrm{CE}} \sim A_{\mathrm{E}}^{-(\beta-1)} \tag{3}$$

where A_{E} is the earthquake rupture area and $(\beta - 1) = b$ in Eq. (2). The equivalent frequency–

From: CELLO, G. & MALAMUD, B. D. (eds) 2006. *Fractal Analysis for Natural Hazards*. Geological Society, London, Special Publications, **261**, 1–9.
0305-8719/06/$15.00

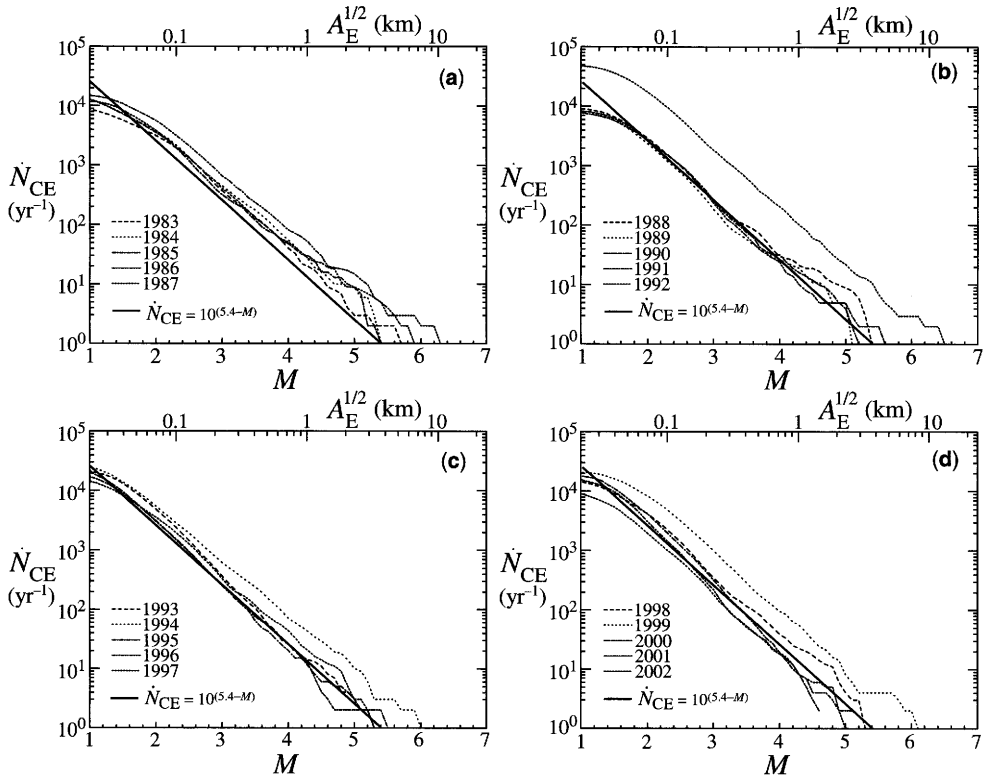

Fig. 1. Cumulative frequency statistics of earthquakes in southern California (figure after Rundle *et al.* 2003). Shown are the cumulative number of earthquakes, $\dot{N}_{CE}$, occurring in southern California, with magnitudes greater than or equal to M as a function of M. Also shown is the equivalent square root of the rupture area, $A_E^{1/2}$. Twenty individual years are considered, with data from the Southern California Seismic Network: (**a**) 1983–1987, (**b**) 1988–1992, (**c**) 1993–1997, (**d**) 1998–2002. The solid straight lines in (**a**) to (**d**) are the Gutenberg–Richter power-law relation (Eq. 2) with $b = 1.0$ and $\dot{a} = 2.5 \times 10^5$ yr^{-1}, fit to all the data from 1983–2002. The larger number of earthquakes in 1987, 1992, 1994, and 1999 can be attributed to the aftershocks of the Whittier–Narrows, Landers, Northridge, and Hector Mine earthquakes, respectively. During the other sixteen years, when there are not a large number of aftershocks, the data closely represent the background seismicity in southern California, and are nearly uniform from year to year, with very similar power-law exponents.

area distribution for Eq. (3) that is noncumulative has a power-law exponent of β, the same as in Eq. (1).

As just one example of Gutenberg–Richter scaling, in Figure 1 we consider regional seismicity in southern California on a yearly basis, as given by Rundle *et al.* (2003). Plotted for each individual year in the period 1983–2002 are the cumulative numbers of earthquakes $\dot{N}_{CE}$ with magnitudes greater than or equal to M as a function of M. Also include is the Gutenberg–Richter power-law relation (Eq. 2) (fit to all data, 1983–2002) with $b = 1.0$ and $\dot{a} = 2.5 \times 10^5$ yr^{-1}, shown as solid straight lines in Figures 1a–d. There is generally good agreement between each individual year's data and the Gutenberg–Richter relation (solid line) for the whole period of record. The exceptions can be attributed to the aftershock sequences of the 1987 Whittier-Narrows, 1992 Landers, 1994 Northridge, and 1999 Hector Mine earthquakes. During the sixteen other years when there are not a large number of aftershocks, the data closely represent the background seismicity in southern California, and are nearly uniform from year to year, with very similar power-law exponents. Earthquakes have been shown to satisfy power-law frequency–size statistics over many regions around the world and over many orders of earthquake magnitude (Frohlich & Davis 1993; Kossobokov *et al.* 2000), although some authors question the validity for the very largest earthquakes (Scholz 1997).

Landslides

The second natural hazard we consider is the landslide, a complex natural phenomenon that constitute a serious hazard in many countries (see also Turcotte *et al.* 2006 in this volume, which discusses landslide statistics in much more detail). Landslides are generally the result of triggers such as intense rainfall or earthquakes, with the trigger resulting in a landslide event that may include anything from just one single landslide up to many tens of thousands. A triggered landslide event can be quantified using landslide inventories, which normally includes a tabulation of landslide areas, spatial position, and landslide type.

Malamud *et al.* (2004) considered the frequency–area statistics of three 'fresh' triggered landslide events. The inventories for each landslide event were substantially complete, consisting of (1) more than 11,000 landslides triggered by the 17 January 1994 Northridge (California) earthquake; (2) more than 4000 landslides triggered by a rapid snowmelt event in the Umbria region of Italy in January 1997; and (3) more than 9000 landslides triggered by heavy rainfall in Guatemala during late October and early November 1998. They considered the probability densities $p(A_L)$ of landslide areas A_L, defined as

$$p(A_L) = \frac{1}{N_{LT}} \frac{\delta N_L}{\delta A_L} \tag{4}$$

where δN_L is the number of landslides with areas between A_L and $A_L + \delta A_L$, and N_{LT} is the total number of landslides in the inventory.

Malamud *et al.* (2004) showed that the three sets of probability densities were in excellent agreement with each other, and correlated well with a three-parameter inverse gamma probability distribution function (pdf), which for medium and large landslide areas can be approximated by

$$p(A_L) \approx \frac{1}{a\Gamma(\beta - 1)} \left[\frac{a}{A_L}\right]^{\beta} \tag{5}$$

where A_L is the area of individual landslides, α and β are constants, and $\Gamma(\beta - 1)$ is the gamma function of $\beta - 1$.

The tail of the probability distribution for large landslide areas is a power-law with exponent β, equivalent to Eq. (1). Malamud *et al.* (2004) used a maximum-likelihood fit of the inverse-gamma distribution to the three sets of landslide probability densities, taking $a = 1.28 \times 10^{-3}\,\mathrm{km}^2$ and $\beta = 2.40$. Thus the power-law exponent for the medium and large landslides (the 'tail' of the distribution) is $\beta = 2.40$. The three inventories considered by Malamud *et al.* (2004) contained 4000–11,000 landslides. To examine further the 'general' landslide distribution given by Eq. (5) Turcotte *et al.* (2006) (in this volume) examined a much smaller, but still substantially complete, inventory of 165 landslides triggered by rainfall in the region of Todi, Central Italy, and found a very similar power-law exponent β.

There is accumulating evidence (for a review, see Guzzetti *et al.* 2002) that the frequency–area distribution of medium and large landslides decays as an inverse power of the landslide area. This behaviour is observed despite large differences in landslide types, sizes, distributions, patterns, and triggering mechanisms.

Wildfires

Our final example of a natural hazard that follows power-law frequency–area statistics to a good approximation is the wildfire. Malamud *et al.* (1998) considered four wildfire data sets from the USA and Australia. The four data sets come from a wide variety of geographic regions with different vegetation types and climates. In each case, the noncumulative number of fires per year plotted as a function of burned fire area A_F correlated well with the power-law relationship (Eq. 1), with $\beta = 1.3$–1.5.

Malamud *et al.* (2005) carried out a comprehensive study of the frequency–area statistics of 88,916 wildfires on United States Forest Service lands in the conterminous USA during the period 1970–2000, examining the statistics both spatially, as a function of ecoregion, and temporally. Ecoregions are land units classified by climate, vegetation, and topography. As the wildfire inventories used were not 'complete' (there are many more 'smaller' wildfires than measured), probability densities as defined in Eq. (4) were not appropriate for the analyses and they used frequency densities $f(A_F)$ defined as

$$f(A_F) = \frac{\delta N_F}{\delta A_F} \tag{6}$$

where A_F is the wildfire burned area, and δN_F the number of wildfires in a 'bin' of width δA_F. The frequency densities $f(A_F)$ are then the number of wildfires per 'unit' bin. The frequency density $f(A_F)$ in Eq. (6) is equal to the probability density $p(A_F)$ introduced in Eq. (4) multiplied by the total number of wildfires in the inventory N_{FT}. For each of eighteen different ecoregions examined in the conterminous USA, Malamud *et al.* (2005) found that the noncumulative number of fires per year plotted as a function of burned fire area A_F

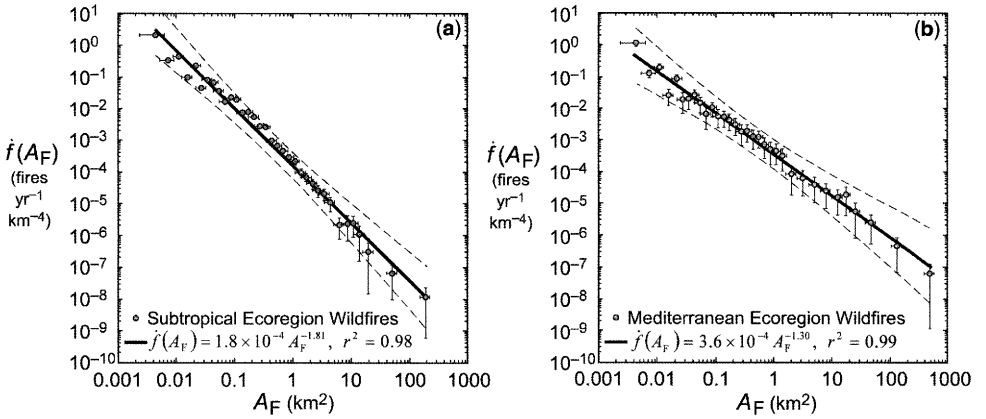

Fig. 2. Normalized frequency–area wildfire statistics for (**a**) *Mediterranean* and (**b**) *Subtropical* ecoregion divisions, for the period 1970–2000 (figure after Malamud *et al.* 2005). Shown (circles) are normalized frequency densities $\hat{f}(A_F)$ (number of wildfires per 'unit bin' of 1 km^2, normalized by database length in years and USFS area within the ecoregion) plotted as a function of wildfire area A_F. Also shown for both ecoregions is a solid line, the best least-squares fit to Eq. (1), with coefficient of determination r^2. Dashed lines represent lower/upper 95% confidence intervals, calculated from the standard error. Horizontal error bars are due to measurement and size binning of individual wildfires. Vertical error bars represent two standard deviations (± 2 s.d.) of the normalized frequency densities $\hat{f}(A_F)$.

correlated well with the power-law relationship (Eq. 1), with $\beta = 1.30-1.81$. Two examples are given in Figure 2, showing the two extremes of values obtained by the authors.

In Figure 2a are presented the frequency–area statistics for 16,423 wildfires in the *Subtropical* ecoregion division (within the southeastern part of the USA) and in Figure 2b, 475 wildfires in the *Mediterranean* ecoregion division (within California, USA). In both cases, excellent correlations are obtained with the power-law relationship (Eq. 1), with $\beta = 1.81 \pm 0.07$ (± 2 s.d.) for the *Subtropical* ecoregion and $\beta = 1.30 \pm 0.05$ (± 2 s.d.) for the *Mediterranean* ecoregion. One of the purposes of this paper is to examine this variability of the power-law exponent β.

A number of other authors (e.g. Niklasson & Granstrom 2000; Minnich 2001; Ricotta *et al.* 2001) have also found good correlations of the frequency–area distributions of wildfires with the power-law relation (1), although others disagree (Cumming 2001; Reed & McKelvey 2002). Millington *et al.* (2006), another chapter in this volume, give a detailed discussion and review of power-law scaling in wildfire areas. In addition to wildfire areas, some authors (Sole & Manrubia 1995*a*, *b*) have found that the frequency–area distributions of clusters of trees in forests also follow power-law statistics.

Considering the many complexities of the initiation and propagation of wildfires, it is remarkable that the frequency–area statistics are similar under a wide variety of environments. The proximity of combustible material varies widely. The behaviour of a particular wildfire depends strongly on meteorological conditions. Fire-fighting efforts extinguish many fires. Despites these complexities, the power-law frequency–area statistics of actual wildfires seems very robust.

Cellular-automata models

Cellular-automata (CA) models are lattice-based models that have simple 'rules', but often exhibit complex behaviour. At each time step, a series of nearest-neighbour rules of interaction are applied, and individual cells are updated in the next step. A brief history of cellular automata is given by Sarkar (2000). A number of 'simple' CA models have been shown to exhibit robust power-law statistics (for reviews see Turcotte 1999; Malamud & Turcotte 2000). We will discuss three of these here, the sandpile, forest-fire, and slider-block models.

We begin with the sandpile model introduced by Bak *et al.* (1988) in the context of his discussions on self-organized criticality. In this model there is a square grid of boxes and at each time step a particle is dropped into a randomly selected box. When a box accumulates four particles, they are redistributed to the four adjacent boxes, or in the case of edge boxes, lost from the grid. Redistributions can lead to further instabilities, with 'avalanches' of particles lost from the edges of the grid. Because of this 'avalanche' behaviour, this was called a 'sandpile' model. This is a cellular-automata

model because the boxes are the cells and the nearest-neighbour redistribution rules constitute the automata. This CA model, and others like it, generate 'avalanches' with a power-law frequency–size distribution, and contains a steady-state 'input', with the 'output' occurring in the 'avalanches'. The noncumulative frequency–area distribution of model avalanches was found to satisfy the power-law distribution given in Eq. (1) with $\beta = 1.0–1.3$ (Bak *et al.* 1988; Kadanoff *et al.* 1989; Turcotte 1997).

A second CA model with robust power-law statistics is the forest-fire model (Bak *et al.* 1990; Drossel & Schwabl 1992*a*, *b*). In the simplest version of this model, a square grid of sites is considered. At each time step either a tree is planted on a randomly chosen site (if the site is unoccupied) or a spark is dropped on the site. If the spark is dropped on a site with a tree, that tree and all adjacent sites with trees are 'burned' in a model 'forest fire'. The firing frequency f is the inverse number of attempted tree drops on the square grid before a model match is dropped on a randomly chosen site. If $f = 1/100$, there have been 99 attempts to plant trees (some successful, some unsuccessful) before a match is dropped at the 100th time step. Two examples of model fires are given in Figure 3. For a broad range of grid sizes and firing frequencies (discussed in more detail in the next section), the frequency–area distribution of the small and medium model fires again satisfies Eq. (1) with $\beta = 1.19$ (Grassberger 2002).

A third CA model that exhibits robust power-law statistics is the slider-block model (Burridge & Knopoff 1967; Carlson & Langer 1989). In this model, an array of slider blocks are connected to a constant velocity driver plate by puller springs and to each other by connector springs. The blocks exhibit stick–slip behaviour as a result of frictional interactions with the plate across which they are pulled. The area is defined to be the number of blocks that participate in a slip event. The frequency–area distribution of smaller and medium slip events again satisfies Eq. (1), with $\beta = 1.0–1.5$ (Carlson & Langer 1989; Huang *et al.* 1992; Carlson *et al.* 1994). This model is deterministic, whereas the sandpile and forest-fire models are stochastic.

A number of authors have discussed each of these CA models in the context of specific natural hazards: the sandpile model with landslides (e.g. Guzzetti *et al.* 2002), the forest-fire model with wildfires (Malamud *et al.* 1998), and the slider-block model with earthquakes (Burridge & Knopoff 1967; Carlson & Langer 1989). In the next section, we will advance an 'explanation' for both the behaviour of the models and natural hazards in terms of the coalescence of growing metastable regions, by introducing the inverse-cascade model in the context of the forest-fire model.

Metastable regions and the inverse-cascade model

Before introducing the inverse-cascade model, we will discuss the role of metastable regions in CA models. A metastable region is the region over which an 'avalanche' spreads once the region is triggered. The role of metastable regions can be illustrated by the forest-fire model. In this model,

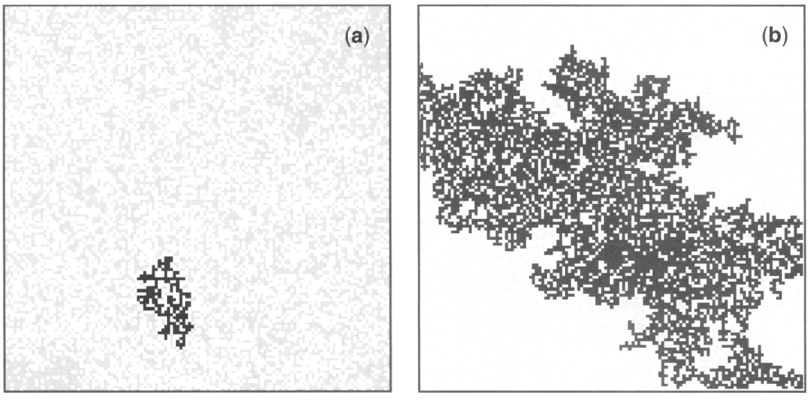

Fig. 3. Two forest-fire model examples using a grid of 128 × 128 cells and a forest-fire run with sparking frequency $1/f = 2000$. The black squares constitute the model forest fires. The light grey squares are unburned trees. The white regions are unoccupied grid points (i.e. no trees). The area of the model fire in (**a**) is $A_F = 204$ trees and in (**b**) $A_F = 5237$ trees; the latter is seen to span the entire grid.

a metastable region is a cluster of trees that will burn when any of the trees is ignited by a match. Thus at any one time, all clusters of trees on the grid are metastable in the sense that each one has the potential to be ignited. We will denote as A_F the area of a cluster, N_F the number of model fires at a given size A_F that burn over time, and $N_{cluster}$ the number of clusters on the grid (at any one time) with area A_F, each of which could potentially burn to give a fire of size A_F. Because the probability that a match will strike a cluster is proportional to its area A_F, then the probability that a cluster of size A_F will burn in a specified time interval, is proportional to the product of the cluster area A_F and the number of clusters $N_{cluster}$, or

$$N_F \sim A_F N_{cluster}. \tag{7}$$

Because the frequency–area distribution satisfies Eq. (1), $N_F \sim A_F^{-\beta}$, it follows from Eq. (7) that

$$N_{cluster} \sim A_F^{-(\beta+1)}. \tag{8}$$

A distribution of fire sizes over time is a power-law with exponent $-\beta$. This implies a distribution of cluster sizes on the grid at one 'snapshot' in time, that is, a power-law with exponent $-(\beta+1)$.

The inverse-cascade model is a relatively simple model that might provides a potential explanation for the power-law frequency–size distributions found in both the CA models and actual natural hazards. To better understand the inverse-cascade model, we continue our discussion in the context of the forest-fire model.

It has been shown (Turcotte *et al.* 1999; Turcotte 1999; Gabrielov *et al.* 1999) that tree clusters grow primarily by coalescence. There are three ways that clusters form on the grid:

(1) A newly planted tree forms a 'single cluster'; in other words there are no adjacent cells containing trees and a cluster of 1 tree is formed.
(2) A tree is planted immediately adjacent to an existing cluster with A_i trees; a new cluster of $(A_i + 1)$ trees is formed.
(3) A newly planted tree bridges the gap between two clusters with A_i and A_j trees; a new cluster is formed with $(A_i + A_j + 1)$ trees.

A detailed study of cluster growth in the forest-fire model by Yakovlev *et al.* (2005) has shown that the last method, cluster coalescence, dominates the cluster growth process. Trees cascade from smaller to larger clusters until they are lost in the fires that destroy the largest clusters, and the cascade is terminated. This is termed an 'inverse cascade', because the flow of trees is from smaller to larger clusters. Turcotte *et al.* (1999) quantified this inverse cascade by introducing a cluster coalescence rate c_{ij}, which is the rate at which N_i clusters of area A_i coalesce with N_j clusters of area A_j. The rate of coalescence c_{ij} is proportional to the cluster numbers N_i and N_j and to the linear dimensions of the clusters r_i and r_j:

$$c_{ij} \sim N_i N_j r_i r_j. \tag{9}$$

We further hypothesize a power-law (fractal) scaling between the linear dimension of a cluster and its area:

$$r_i \sim A_i^{\xi}, \qquad r_j \sim A_j^{\xi}. \tag{10}$$

For Euclidian clusters, for example a 'circle' of occupied sites, then $\xi = 1/2$. There are two contributions to the fractal structure of clusters. The first is due to the density of trees in the cluster. If the density of trees is low, then the cluster will have a larger radius relative to the number of trees in the cluster. The second effect is the irregularity of the boundary of the cluster. If the cluster has thin arms (tentacles) that reach out, these will result in an increased rate of coalescence.

The studies of Gabrielov *et al.* (1999) and Yakovlev *et al.* (2005) have shown that, at any given time, the number of clusters on the grid $N_{cluster}$ with area A_F is given by

$$N_{cluster} \sim A_F^{-(\xi+1.5)}. \tag{11}$$

Comparing Eqs. (8) and (11), we obtain

$$\alpha = \xi + 0.5. \tag{12}$$

The power-law exponent β of the scaling relation between the number of fires N_F and A_F is $(\xi + 0.5)$. From Eqs. (1) and (12) we have

$$N_F \sim A_F^{-\beta} \sim A_F^{-(\xi+0.5)}. \tag{13}$$

Up to this point we have been examining the scaling of the frequency–area distributions of model fires and clusters. We now examine the fractal nature of the two-dimensional clusters and fires themselves in the forest-fire model, by associating the values of ξ just discussed with the fractal dimension D of the tree clusters and the model fires.

The statistical fractal structure of fires and clusters of area A_F are identical. This association is illustrated by the fractal construction given in Figure 4. At first order $i = 1$ (Fig. 4a) we have a single tree with linear size $r_1 = 1$ and area $A_1 = 1$ tree. At second order $i = 2$, we add four trees in the adjacent sites, as shown in Figure 4b. The

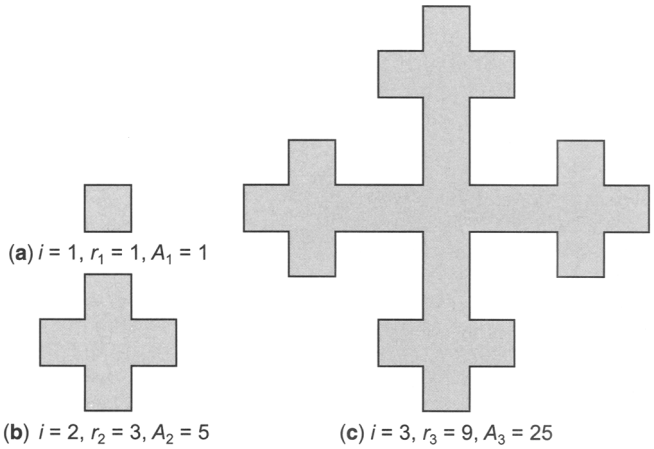

Fig. 4. Deterministic fractal construction illustrating the dependence of the rate of coalescence c_{ij} on areas A_i and A_j. In (**a**) we consider a single 'tree' so that linear size $r_1 = 1$ and area $A_1 = 1$ tree. In (**b**) we fill the four adjacent sites with trees so that the linear size is now $r_2 = 3$ and area is $A_2 = 5$ trees. In (**c**) we repeat this construction using the structure given in (**b**) so that linear size is now $r_3 = 9$ and area $A_3 = 25$ trees. The fractal dimension of this construction is $D = \ln 5/\ln 3 = 1.46$.

linear size is now $r_2 = 3$ and area $A_2 = 5$ trees. At third order $i = 3$ we take four of the second-order structures from Figure 4b, in analogy with the transition from Figures 4a to b, with the result given in Figure 4c. The linear size is now $r_3 = 9$ with area $A_3 = 25$ trees. From Eq. (10) we have

$$\left(\frac{A_i}{A_j}\right)^{\xi} = \frac{r_i}{r_j}. \tag{14}$$

If we take $A_i = A_2 = 5$, $A_j = A_1 = 1$, $r_i = r_2 = 3$, $r_j = r_1 = 1$ for our fractal construction, we then have

$$5^{\xi} = 3 \tag{15}$$

or

$$\xi = \frac{\ln 3}{\ln 5} \approx 0.683. \tag{16}$$

The fractal dimension D of this construction can be defined as (Turcotte 1997)

$$D = \frac{\ln (A_j/A_i)}{\ln (r_j/r_i)} = \frac{\ln 5}{\ln 3} \approx 1.465. \tag{17}$$

If we compare Eq. (16) to Eq. (17), we have

$$\xi = \frac{1}{D}. \tag{18}$$

Although this result was derived for the particular fractal construction illustrated in Figure 4, it is a general result relating r_i, the linear dimension of a fractal object, to its area A_i.

Substitution of Eq. (18) into Eq. (13) gives

$$\beta = 0.5 + \frac{1}{D}. \tag{19}$$

Thus we have related the power-law exponent β of the frequency–area distribution of model fires to the fractal dimension D of the tree clusters. The fractal structure in Figure 4 emphasizes the irregularity of the boundary of the cluster, which dominates over tree density in contributing to high rates of coalescence. This irregularity is also illustrated in the model fires given in Figure 3. Low fractal dimensions (D small) lead to large collision rates and fewer large clusters and fires (i.e. small β) in the model. If the clusters are Euclidian, for example, circles of filled sites, the cluster fractal dimension is $D = 2$. From Eq. (19) this would give $\beta = 1$, that is, $N \sim A^{-1}$, a critical (i.e. power-law) dependence often associated with 'self-organized criticality' (Turcotte 1999).

A very comprehensive numerical study of the same two-dimensional forest-fire model that we have considered in this paper has been given by Grassberger (2002). He considered grid sizes up to $N_g = 65{,}536 \times 65{,}536 \approx 4.295 \times 10^9$ cells, and firing frequencies as small as $f = 1/256{,}000$. Under a wide range of conditions, he found that the frequency–area distribution of model fires was well approximated by Eq. (1), taking $\beta = 1.19$. From Eq. (19), this corresponds to a cluster fractal

dimension of $D = 1.45$. It is interesting to note that the fractal construction illustrated in Figure 4 has a fractal dimension $D = 1.46$.

In Figure 2 we presented frequency–area statistics for wildfires in two different ecoregions in the USA. Although both data sets showed excellent correlation with the power-law relationship (Eq. 1), the exponents were quite different. One potential explanation for these differences would be a variation in the fractal dimension (if one exists) of the combustible materials in the two regions. In the *Mediterranean* ecoregion division we have $\beta = 1.30$, and from Eq. (19) the required 'cluster' fractal dimension is $D = 1.25$. In the *Subtropical* ecoregion division we have $\beta = 1.81$, and from Eq. (19) $D = 0.76$. Because this is less then $D = 1.0$, it does not define a cluster. A two-dimensional cluster requires that $1.0 < D \leq 2.0$. From Eq. (19) we therefore require $1.0 < \beta \leq 1.5$. Because $\beta = 1.81$ for the subtropical ecoregion, the cascade model cannot explain the power-law scaling of fire occurrences.

Discussion and conclusions

In this paper we have considered the frequency–area statistics of three natural hazards: earthquakes, landslides, and wildfires. In each case, the data can be well characterized by robust power laws. We have also considered three cellular-automata models. In each case 'avalanches' occur and the frequency–area distributions of the avalanches are well approximated by power laws. In order to advance a potential explanation for the robust power-law behaviour observed in both data and CA models, we consider an inverse-cascade model for metastable cluster coalescence. We find that this cascade model also gives robust power-law frequency–area statistics with the power-law exponent controlled by the fractal dimension of the clusters. The cascade model requires that the power-law exponent β be in the range $1.0 < \beta \leq 1.5$. Thus the inverse-cascade model provides a satisfactory basis for the behaviour of the forest-fire CA model.

Many data sets for real wildfires of frequency–area distributions also fall into the required range $1.0 < \beta \leq 1.5$ (e.g. the *Mediterranean* ecoregion, Fig. 2b); however, others clearly do not (e.g. the *Subtropical* ecoregion, Fig. 2a). Of the eighteen ecoregion divisions examined by Malamud *et al.* (2005), half of them have $1.3 < \beta \leq 1.5$ and the other half $1.5 < \beta \leq 1.8$. We conclude that the cascade model does not provide a full explanation for the power-law frequency–area statistics of actual wildfires. This is not surprising, because the spread of actual wildfires is much more complex than the cellular-automata forest-fire model. Nevertheless, the robust agreement of wildfire data with power-law scaling is striking.

The contributions of author D.L.T. were partially supported by NSF Grant No. ATM 0327558 and the contributions of author B.D.M. were partially supported by the European Commission's Project No. 12975 (NEST) 'Extreme events: Causes and consequences (E2-C2)'.

References

AKI, K. 1981. A probabilistic synthesis of precursory phenomena. *In*: SIMPSON, D. W. & RICHARDS, P. G. (eds) *Earthquake Prediction*. Maurice Ewing Series **4**. American Geophysical Union, Washington, D.C., 566–574.

BAK, P., TANG, C. & WIESENFELD, K. 1988. Self-organized criticality. *Physical Review A*, **38**, 364–374.

BAK, P., CHEN, K. & TANG, C. 1990. A forest-fire model and some thoughts on turbulence. *Physics Letters A*, **147**, 297–300.

BURRIDGE, R. & KNOPOFF, L. 1967. Model and theoretical seismicity. *Seismological Society of America Bulletin*, **57**, 341–371.

CARLSON, J. M. & LANGER, J. S. 1989. Mechanical model of an earthquake fault. *Physical Review A*, **40**, 6470–6484.

CARLSON, J. M., LANGER, J. S. & SHAW, B. E. 1994. Dynamics of earthquake faults. *Reviews of Modern Physics*, **66**, 657–670.

CHAPMAN, C. R. 2004. The hazard of near-Earth asteroid impacts on earth. *Earth and Planetary Sciences Letters*, **222**, 1–15.

CHAPMAN, C. R. & MORRISON, D. 1994. Impacts on the Earth by asteroids and comets: assessing the hazard. *Nature*, **367**, 33–40.

CUMMING, S. G. 2001. A parametric model of the fire size distribution. *Canadian Journal of Forest Research*, **31**, 1297–1303.

DROSSEL, B. & SCHWABL, F. 1992*a*. Self-organized criticality in a forest-fire model. *Physica A*, **191**, 47–50.

DROSSEL, B. & SCHWABL, F. 1992*b*. Self-organized critical forest-fire model. *Physical Review Letters*, **69**, 1629–1632.

FROHLICH, C. & DAVIS, S. D. 1993. Teleseismic b values; or, much ado about 1.0. *Journal of Geophysical Research*, **98**(B1), 631–644.

GABRIELOV, A., NEWMAN, W. I. & TURCOTTE, D. L. 1999. An exactly soluble hierarchical clustering model: inverse cascades, self-similarity, and scaling. *Physical Review E*, **60**, 5293–5300.

GRASSBERGER, P. 2002. Critical behavior of the Drossel–Schwabl forest fire model. *New Journal of Physics*, **4**, 17.1–17.15.

GUTENBERG, B. & RICHTER, C. F. 1954. *Seismicity of the Earth and Associated Phenomena*, 2nd edn. Princeton University Press, Princeton.

GUZZETTI, F., MALAMUD, B. D., TURCOTTE, D. L. & REICHENBACH, P. 2002. Power-law correlations

of landslide areas in central Italy. *Earth and Planetary Science Letters*, **195**, 169–183.

HUANG, J., NARKOUNSKAIA, G. & TURCOTTE, D. L. 1992. A cellular-automata, slider-block model for earthquakes: 2. Demonstration of self-organized criticality for a 2-D system. *Geophysical Journal International*, **111**, 259–269.

KADANOFF, L. P., NAGEL, S. R., WU, L. & ZHOU, S. M. 1989. Scaling and universality in avalanches. *Physical Review*, **A39**, 6524–6537.

KOSSOBOKOV, V. G., KEILIS-BOROK, V. I., TURCOTTE, D. L. & MALAMUD, B. D. 2000. Implications of a statistical physics approach for earthquake hazard assessment and forecasting. *Pure and Applied Geophysics*, **157**, 2323–2349.

MALAMUD, B. D. 2004. Tails of natural hazards. *Physics World*, **17**, 31–35.

MALAMUD, B. D. & TURCOTTE, D. L. 2000. Cellular-automata models applied to natural hazards. *IEEE Computing in Science and Engineering*, **2**, 42–51.

MALAMUD, B. D. & TURCOTTE, D. L. 2006. The applicability of power-law frequency statistics to floods. *Journal of Hydrology*, **322**, 160–180.

MALAMUD, B. D., TURCOTTE, D. L. & BARTON, C. C. 1996. The 1993 Mississippi River flood: a one-hundred or a one-thousand year event? *Environmental and Engineering Geology*, **2**, 479–486.

MALAMUD, B. D., MOREIN, G. & TURCOTTE, D. L. 1998. Forest fires: an example of self-organized critical behavior. *Science*, **281**, 1840–1842.

MALAMUD, B. D., TURCOTTE, D. L., GUZZETTI, F. & REICHENBACH, P. 2004. Landslide inventories and their statistical properties. *Earth Surface Processes and Landforms*, **29**, doi 10.1002/esp.1064, 687–711.

MALAMUD, B. D., MILLINGTON, J. D. A. & PERRY, G. L. W. 2005. Characterizing wildfire regimes in the USA. *Proceedings of the National Academy of Sciences*, **102**, 4694–4699.

MILLINGTON, J. D. A., PERRY, G. L. W. & MALAMUD, B. D. 2006. Models, data and mechanisms: quantifying wildfire regimes. *In*: CELLO, G. & MALAMUD, B. D. (eds) *Fractal Analysis for Natural Hazards*. Geological Society, London, Special Publications, **261**, 155–167.

MINNICH, R. A. 2001. An integrated model of two fire regimes. *Conservation Biology*, **15**, 1549–1553.

NIKLASSON, M. & GRANSTROM, A. 2000. Numbers and sizes of fires: long-term spatially explicit fire history in a Swedish boreal landscape. *Ecology*, **81**, 1484–1499.

PYLE, D. M. 2000. Sizes of volcanic eruptions. *In*: SIGURDSSON, H., HOUGHTON, B., RYMER, H., STIX, J. & MCNUTT, S. (eds) *Encyclopedia of Volcanoes*. Academic Press, San Diego, 263–269.

REED, W. J. & MCKELVEY, K. S. 2002. Power law behaviour and parametric models for the size-distribution of forest fires. *Ecological Modelling*, **150**, 239–254.

RICOTTA, C., AVENA, G. & MARCHETTI, M. 1999. The flaming sandpile: self-organized criticality and wildfires. *Ecological Modelling*, **119**, 73–77.

RICOTTA, C., ARIANOUTSOU, M. *ET AL.* 2001. Self-organized criticality of wildfires ecologically revisited. *Ecological Modelling*, **141**, 307–311.

RUNDLE, J. B., TURCOTTE, D. L., SHCHERBAKOV, R., KLEIN, W. & SAMMIS, C. 2003. Statistical physics approach to understanding the multiscale dynamics of earthquake fault systems. *Reviews of Geophysics*, **41**, article number 1019, doi:10.1029/2003RG000135, 5-1–5-30.

SARKAR, P. 2000. A brief history of cellular automata. *ACM Computing Surveys*, **32**, 80–107.

SCHOLZ, C. H. 1997. Size distributions for large and small earthquakes. *Seismological Society of America Bulletin*, **87**, 1074–1077.

SOLE, R. V. & MANRUBIA, S. C. 1995*a*. Self-similarity in rain forests: Evidence for a critical state. *Physical Review E*, **51**, 6250–6353.

SOLE, R. V. & MANRUBIA, S. C. 1995*b*. Are rainforests self-organized in a critical state? *Journal of Theoretical Biology*, **173**, 31–40.

TURCOTTE, D. L. 1994. Fractal theory and the estimation of extreme floods. *Journal of Research of the National Institute of Standards and Technology*, **99**, 377–389.

TURCOTTE, D. L. 1997. *Fractals and Chaos in Geology and Geophysics*, 2nd edn. Cambridge University Press, Cambridge.

TURCOTTE, D. L. 1999. Self-organized criticality. *Reports on Progress in Physics*, **62**, 1377–1429.

TURCOTTE, D. L. & GREENE, L. 1993. A scale-invariant approach to flood-frequency analysis. *Stochastic Hydrology and Hydraulics*, **7**, 33–40.

TURCOTTE, D. L. & MALAMUD, B. D. 2002. Earthquakes as a complex system. *In*: LEE, W. H. K., KANAMORI, H., JENNINGS, P. C. & KISSLINGER, C. (eds) *International Handbook of Earthquake & Engineering Seismology*. Academic Press, London, 209–227.

TURCOTTE, D. L., MALAMUD, B. D., GUZZETTI, F. & REICHENBACH, P. 2006. A general landslide distribution applied to a small inventory in Todi, Italy. *In*: CELLO, G. & MALAMUD, B. D. (eds) *Fractal Analysis for Natural Hazards*. Geological Society, London, Special Publications, **261**, 105–111.

TURCOTTE, D. L., MALAMUD, B. D., MOREIN, G. & NEWMAN, W. I. 1999. An inverse-cascade model for self-organized critical behavior. *Physica A*, **268**, 629–643.

YAKOVLEV, G., NEWMAN, W. I., TURCOTTE, D. L. & GABRIELOV, A. 2005. An inverse cascade model for self-organized complexity and natural hazards. *Geophysical Journal International*, **163**, 433–442.